frontiers | Frontiers in Immunology

TYPE Original Research
PUBLISHED 25 September 2023
DOI 10.3389/fimmu.2023.1243851



OPEN ACCESS

EDITED BY
Emilia Lecuona,
Northwestern University, United States

REVIEWED BY
Misagh Rajabinejad,
Mazandaran University of Medical Sciences, Iran
Ricardo Sanchez-Rodriguez,
University of Padua, Italy

*CORRESPONDENCE
Masashi Tachibana
tacci@phs.osaka-u.ac.jp

RECEIVED 21 June 2023
ACCEPTED 07 September 2023
PUBLISHED 25 September 2023

CITATION
Xie Z, Zhou H, Obana M, Fujio Y, Okada N and Tachibana M (2023) Myeloid-derived suppressor cells exacerbate poly(I:C)-induced lung inflammation in mice with renal injury and older mice.
*Front. Immunol.* 14:1243851.
doi: 10.3389/fimmu.2023.1243851



# Myeloid-derived suppressor cells exacerbate poly(I:C)-induced lung inflammation in mice with renal injury and older mice

Zhiqi Xie[1,2], Haoyang Zhou[2], Masanori Obana[3,4,5,6], Yasushi Fujio[3,4,5], Naoki Okada[2] and Masashi Tachibana[2,6,7]*

[1]Key Laboratory of Novel Targets and Drug Study for Neural Repair of Zhejiang, School of Medicine, Hangzhou City University, Hangzhou, Zhejiang, China, [2]Project for Vaccine and Immune Regulation, Graduate School of Pharmaceutical Sciences, Osaka University, Osaka, Japan, [3]Laboratory of Clinical Science and Biomedicine, Graduate School of Pharmaceutical Sciences, Osaka University, Osaka, Japan, [4]Integrated Frontier Research for Medical Science Division, Institute for Open and Transdisciplinary Research Initiatives (OTRI), Osaka University, Osaka, Japan, [5]Center for Infectious Disease Education and Research (CiDER), Osaka University, Osaka, Japan, [6]Global Center for Medical Engineering and Informatics, Osaka University, Osaka, Japan, [7]Laboratory of Biochemistry and Molecular Biology, Graduate School of Pharmaceutical Sciences, Osaka University, Osaka, Japan

Viral pneumonia is a global health burden with a high mortality rate, especially in the elderly and in patients with underlying diseases. Recent studies have found that myeloid-derived suppressor cells (MDSCs) are abundant in these patient groups; however, their roles in the progression of viral pneumonia remain unclear. In this study, we observed a substantial increase in MDSCs in a mouse model of renal ischemia/reperfusion (I/R) injury and in older mice. When intranasal polyinosinic-polycytidylic acid (poly(I:C)) administration was used to mimic viral pneumonia, mice with renal I/R injury exhibited more severe lung inflammation than sham mice challenged with poly(I:C). In addition, MDSC depletion attenuated lung inflammation in mice with I/R injury. Similar results were obtained in older mice compared with those in young mice. Furthermore, adoptive transfer of in *vitro*-differentiated MDSCs exacerbated poly(I:C)-induced lung inflammation. Taken together, these experimental results suggest that the increased proportion of MDSCs in mice with renal I/R injury and in older mice exacerbates poly(I:C)-induced lung inflammation. These findings have important implications for the treatment and prevention of severe lung inflammation caused by viral pneumonia.

KEYWORDS

**MDSC, poly(I:C), lung inflammation, aging, renal ischemia/reperfusion injury**

# 1 Introduction

Viral lung infections are a considerable global health burden. In patients with highly pathogenic respiratory viral infections, pneumonia and the resulting acute respiratory distress syndrome, septic shock, and multiple organ failure are major risk factors for severe and fatal illnesses (1–3). Multiple patient surveys from the 2003 severe acute respiratory syndrome (SARS) and coronavirus disease 2019 (COVID-19) outbreaks revealed that elderly patients, as well as those with underlying medical conditions, such as kidney disease, diabetes, hypertension, cancer, and immunosuppression, are prone to developing severe illness (4–6). Because these individuals are often immunocompromised, the immune response to antiviral therapy may lead to death due to complications related to the underlying disease. For example, patients with diabetes and hypertension have a sustained increase in proinflammatory cytokines caused by a dysregulated immune response, which may skew the antiviral response toward an inflammatory response associated with cytokine storms, tissue damage, and respiratory failure (7–9). Older patients with chronic kidney disease, who are most at risk for death due to COVID-19, often have immune senescence and immunosuppressive conditions that hinder the approaches used to combat SARS-CoV-2 infection (10). Unfortunately, the cascade of pathological and immune events and the key mechanisms involved in the aggravation of viral pneumonia remain unclear.

Myeloid-derived suppressor cells (MDSCs) are immune cells with suppressive functions that have received considerable attention in recent decades. MDSCs are a heterogeneous group of myeloid cells that can be classified as $CD11b^{+}Ly\text{-}6G^{-}Ly\text{-}6C^{hi}$ monocytic MDSCs (M-MDSCs) and $CD11b^{+}Ly\text{-}6G^{+}Ly\text{-}6C^{int}$ polymorphonuclear MDSCs (PMN-MDSCs) based on their morphology and expression of surface markers in mice (11). M-MDSCs suppress T-cell proliferation via arginase 1 and inducible nitric oxide synthase (iNOS), whereas PMN-MDSCs exert inhibitory effects through arginase 1 and reactive oxygen species (ROS) (12). Although MDSCs were originally described in patients with cancer, recent studies have highlighted their important roles in regulating immune responses in other pathological conditions, including infection, transplantation, and autoimmune diseases (13, 14). In addition, there is compelling evidence that aging increases the number of circulating MDSCs in humans and mice (15), whereas $CD11b^{+}Gr\text{-}1^{+}$ cells isolated from the spleens of older mice can effectively inhibit T-cell proliferation and activity (16). Other studies have shown that MDSCs can exert suppressive effects through various pathways that ameliorate acute kidney injury or diabetic kidney disease (17, 18). Together, these observations suggest that MDSCs may prevent excessive inflammation caused by aging and kidney disease. Paradoxically, MDSCs can also promote tissue degeneration and increase the risk of infection complications (19, 20), and exacerbate kidney damage (21). Furthermore, MDSCs can display features of proinflammatory cells and contribute toward hyperinflammation under certain conditions (22–24), suggesting that the behavior of MDSCs depends on the context of the disease.

Several studies have highlighted the potential role of MDSCs in viral infections, including influenza A virus (IAV), hepatitis C virus (HCV), and SARS-CoV-2 (25–28). In patients with COVID-19, MDSC expansion after infection correlates with disease severity and mortality (23). Available data also suggests a direct role for MDSCs in exacerbating respiratory viral infections (27). As increased morbidity and mortality rates are consistently observed in aging individuals and in those with chronic diseases during viral infections, the increased frequency of MDSCs in such individuals may play a detrimental role in the progression of viral pneumonia. In this study, older mice and those with renal ischemia/reperfusion (I/R) injury were challenged with polyinosinic-polycytidylic acid (poly(I:C)) as a viral RNA analog to induce lung inflammation. We aimed to unravel the role of MDSCs in these models of poly(I:C)-induced lung inflammation and explore its implications in the treatment and prevention of severe lung inflammation caused by viral pneumonia in aging individuals and in those with chronic diseases.

# 2 Materials and methods

## 2.1 Mice

Inbred male C57BL/6J mice (6–8 weeks old) were purchased from Japan SLC (Shizuoka, Japan) and were aged over 24 weeks in our facility. All animals were bred and maintained under pathogen-free conditions.

## 2.2 Preparation of poly(I:C)

High-molecular-weight poly(I:C) (InvivoGen, CA, USA) was prepared according to the manufacturer's instructions. Briefly, endotoxin-free water (provided by the manufacturer) was added to poly(I:C) for a final concentration of 4 mg/mL; the solution was incubated in a hot water bath (65–70°C) for 10 min, and allowed to cool slowly to room temperature (approximately 25°C) to ensure proper annealing. The poly(I:C) solution was then aliquoted and stored at −20°C. Before use, the poly(I:C) solution was diluted and vortexed to ensure thorough mixing.

## 2.3 Murine model of poly(I:C)-induced pneumonia

Male C57BL/6J mice (6–8 weeks old; young mice, or over 24 weeks old; older mice) were anesthetized using isoflurane. Different doses (20, 50, and 100 μg) of poly(I:C) in 50 μL sterile phosphate-buffered saline (PBS) or PBS alone were administered intranasally (*i.n.*) twice through both nostrils alternately (29, 30). Mice received seven poly(I:C) (or PBS) administrations, with a 24 h rest period between each administration. Anti-Ly-6G (clone1A8, 2 mg/kg; BioXCell, NH, USA) and anti-Ly-6C (clone: Monts 1, 2 mg/kg;

BioXCell) were administered by intraperitoneal (*i.p.*) injection one day before poly(I:C) challenge, with one more dose injected after three days. Mice were sacrificed 7 days after poly(I:C) injection and retro-orbital blood (approximately 75 µL) was collected for flow cytometry analysis. Blood cell counts were determined using an XT-2000i automated hematology analyzer (Sysmex, Kobe, Japan). Lungs and brochoalveolar lavage fluid (BALF) were obtained for further analysis.

## 2.4 Murine model of renal I/R injury

The mouse model of renal I/R injury was established as described previously (31, 32). Briefly, 6–8 weeks old male mice were anesthetized using isoflurane. A left unilateral flank incision was made and renal pedicle dissection was performed. A microvascular clamp (Natsume Seisakusho, Japan) was placed on the renal pedicle for 22 min while the animal was kept at a constant temperature and adequately hydrated. The clamp was then removed, the wound was sutured, and the mice were allowed to recover. After seven days, retro-orbital blood or spleen samples were collected to evaluate MDSC levels. Anti-Ly-6C and Anti-Ly-6G antibodies and poly(I:C) were administered.

## 2.5 Collection of bronchoalveolar lavage fluid

After sacrifice, an incision was made in the abdominal cavity of mice and a microvascular clamp was placed in the bronchus of the left lung. BALF was obtained by inserting a 20-gauge catheter into the trachea, through which 0.5 mL of cold Hank's Balanced Salt Solution (HBSS; Gibco, USA) was flushed back and forth three times. BALF was centrifuged at 330 × *g* for 5 min at 4°C. Cell-free supernatants were used to measure cytokine concentrations using Bio-Plex. The BALF cell pellet was treated with red cell lysis buffer and resuspended in Hank's Balanced Salt Solution (HBSS) supplemented with 2% fetal bovine serum (FBS) (2% FBS/HBSS; Gibco, CA, USA) for cell counting and flow cytometry analysis.

## 2.6 Quantitative reverse transcription polymerase chain reaction (qRT-PCR)

Total RNA was isolated from $CD11b^+Gr\text{-}1^+$ cells purified from murine splenocytes using a JSAN cell sorting instrument (KS-Techno, Chiba, Japan) with TRIzol reagent. cDNA was synthesized using a QuantiTect reverse transcription kit (Qiagen, Hilden, Germany) according to the manufacturer's instructions. qRT-PCR was performed using SYBR Premix Ex Taq (Tli RNaseH Plus; TaKaRa, Tokyo, Japan) on a CFX96 Touch Real-Time PCR Detection System (Bio-Rad, CA, USA). The specific primer sequences used are listed in Table S1. Glyceraldehyde 3-phosphate dehydrogenase (*Gapdh*) was used as a reference gene and the relative expression of other genes was calculated using the $2^{-\Delta\Delta Ct}$ method.

## 2.7 Flow cytometry analysis

Cells were pelleted, washed with 2% FBS/HBSS, blocked with TruStain fcX (anti-mouse CD16/32) antibodies (BioLegend, CA, USA) for 5 min, and then stained with the following antibodies for 15 min at 4°C: APC anti-mouse CD11b, Pacific Blue anti-mouse Gr-1, APC-Cy7 anti-mouse Ly-6C, FITC anti-mouse Ly-6G, APC anti-mouse CD3ε, Pacific Blue anti-mouse CD4, PE anti-mouse NK1.1, and FITC anti-mouse CD8α (BioLegend). The cells were then washed and resuspended in 2% FBS/HBSS. Shortly before performing measurements, a 7-amino actinomycin D viability staining solution (BioLegend) was added to each sample to stain dead cells. Flow cytometry analysis was performed using a BD FACSCanto II flow cytometer (BD Biosciences, NJ, USA). Data were analyzed using the FlowJo software (version 10.7.0, BD Biosciences). The gating strategy used for flow cytometry analysis was as follows: monocytes ($7AAD^-CD45^+CD11b^+Ly\text{-}6G^-Ly\text{-}6C^{hi}$), neutrophils ($7AAD^-CD45^+CD11b^+Ly\text{-}6G^+Ly\text{-}6C^{int}$), $CD4^+$ T cells ($7AAD^-CD45^+CD3\varepsilon^+CD4^+NK1.1^-$), $CD8^+$ T cells ($7AAD^-CD45^+CD3\varepsilon^+CD8\alpha^+NK1.1^-$), and NK cells ($7AAD^-CD45^+CD3\varepsilon^-NK1.1^+$) (Figure S1A).

## 2.8 Histopathological examination

The left lungs were removed from euthanized mice, fixed in 10% formalin, and sent to the Kyoto Institute of Nutrition & Pathology for paraffin embedding. Whole lungs were cut into 4 µm sections, stained with hematoxylin and eosin (H&E), and imaged using the SLIDEVIEW VS200 Imaging System (EVIDENT, Tokyo, Japan). Digital images were imported into the HALO software (Indica Labs) for analysis. Regions of interest around the relevant areas in each slide were annotated manually and lung sections were divided into normal and inflamed areas using the Indica Labs' Area Quantification module (Version 1.0). Nuclear cells in the inflamed areas (infiltrating inflammatory cells) were automatically counted using the CytoNuclear v2.0.9 analysis module (Figure S1B).

## 2.9 Bio-Plex cytokine analysis

To detect multiple cytokines in BALF, the Bio-Plex Pro mouse cytokine assay (23-Plex Group I; Bio-Rad) was performed using a Luminex-xMAP/Bio-Plex 200 System with the Bio-Plex Manager 6.2 software (Bio-Rad). Cytokine levels were measured using a cytometric magnetic bead-based assay according to the manufacturer's instructions.

## 2.10 Statistical analysis

Shapiro-Wilk normality test was performed to analyze the normal (Gaussian) distribution of data. A $p$-value >0.05 indicated a normal distribution. Subsequently, significant differences were assessed using the Student's $t$-test or one-way analysis of variance (ANOVA) using the GraphPad Prism (GraphPad Software). $P$ values <0.05 were considered statistically significant.

# 3 Results

## 3.1 MDSCs aggravate poly(I:C)-induced lung inflammation in mice with renal I/R injury

Poly(I:C), a synthetic analog of double-stranded RNA, is present in some viruses and is, therefore, widely used to model viral pneumonia (33). Upon binding to toll-like receptor 3 (TLR3), retinoic acid-inducible gene I protein (RIG-I), melanoma differentiation-associated gene 5 (MDA5), and poly(I:C) selectively activate innate immune signaling pathways leading to inflammation (34). First, we aimed to elucidate the importance of MDSCs in poly(I:C)-induced lung inflammation using a mouse model of acute renal I/R injury. A substantial increase in both MDSC subsets was observed in mice with renal I/R injury (Figure 1A) and $CD11b^+Gr\text{-}1^+$ MDSCs showed increased expression of the immunosuppression-associated genes, *Arg1*, *Nos2*, and *Cybb* (Figure 1B).

Repetitive intranasal administration of poly(I:C) significantly increased the number of $CD45^+$ cells in BALF (Figures 1C, D). The increase in total cellularity in BALF was caused by significant monocyte, neutrophil, $CD4^+$ T cell, $CD8^+$ T cell, and NK cell infiltration (Figure 1D). Notably, the number of inflammatory cells in BALF samples harvested from mice with I/R injury mice was significantly increased compared with that in sham mice.

To elucidate whether the effects induced by poly(I:C) in I/R-injured mice depended on MDSCs, I/R-injured mice were treated with anti-Ly-6C and anti-Ly-6G antibodies to deplete circulating MDSCs. Almost all M-MDSCs and total PMN-MDSCs were depleted from the blood (Figure S2). In addition, MDSC-depleted I/R-injured mice displayed reduced inflammatory cell infiltration, especially for monocytes, neutrophils, $CD4^+$ T cells, and $CD8^+$ T cells (Figure 1D).

Histological analysis of the lungs was performed to better understand the pathology induced by poly(I:C). Marked perivascular and moderate peribronchiolar interstitial inflammatory infiltrate was observed in poly(I:C)-treated sham mice (Figures 1E, S3). A more severe inflammatory infiltrate was observed in I/R injured mice and the inflammatory infiltrate in I/R-injured mice was slightly lower under MDSC-depleted conditions (Figures 1E, F). These results suggest that the frequency of MDSCs is increased in mice with renal I/R injury and aggravates poly(I:C)-induced lung inflammation.

## 3.2 MDSCs aggravate poly(I:C)-induced lung inflammation in older mice

Next, we assessed the role of MDSCs in poly(I:C)-induced lung inflammation in older mice. Consistent with previous reports, older mice showed an increase in both MDSC subsets compared to young mice (Figure 2A). In addition, $CD11b^+Gr\text{-}1^+$ MDSCs isolated from older mice showed increased *Arg1*, *Nos2*, and *Cybb* expression compared to those isolated from young mice (Figure 2B). Older mice also showed a significant increase in the number of $CD45^+$ cells in BALF compared to young mice with poly(I:C) challenge, similar to mice with I/R injury (Figures 2C, D). This increase in total cellularity in BALF samples from older mice was caused by significant neutrophil, $CD4^+$ T-cell, and $CD8^+$ T-cell infiltration. Conversely, MDSC depletion significantly decreased the levels of all analyzed cells in older mice (Figure 2D). No significant reduction in total $CD45^+$ cells was observed in young mice; only a decrease in neutrophils and NK cells was noted (Figure 2D). Analysis of lung peribronchial and perivascular inflammatory cells from lung sections revealed more severe inflammatory infiltrate in older mice than in young mice (Figures 2E, F, S4), whereas MDSC depletion reduced poly(I:C)-induced lung inflammation in older mice to the same level as in young mice. Together, these results suggest that MDSCs are upregulated in older mice and aggravate poly(I:C)-induced lung inflammation.

## 3.3 Adoptive transfer of MDSCs aggravates poly(I:C)-induced lung inflammation

To verify the direct effect of MDSCs on poly(I:C)-induced lung inflammation, *in vitro* MDSCs were adoptively transferred into mice in an intravenous manner and the consequences of inflammation were studied. *In vitro* MDSCs were differentiated from BM cells with GM-CSF stimulation, as described previously ($CD11b^+Gr\text{-}1^+$ MDSC purity over 90%, Figure S5A) (35, 36). These cells displayed higher *Arg1*, *Nos2*, and *Cybb* expression than BM cells (Figure S5B) and potently inhibited $CD8^+$ T-cell proliferation (Figure S5C).

Intranasal poly(I:C) administration dose-dependently increased inflammatory cell infiltration into the lungs in both the PBS- and MDSC-transfer groups. The adoptive transfer of MDSCs significantly increased BALF $CD45^+$ cell numbers, even in the absence of poly(I:C), mainly due to $CD4^+$ T-cell and neutrophil infiltration into the lung. When poly(I:C) was administered, monocyte and $CD8^+$ T-cell infiltration also increased (Figures 3A, B). Analysis of lung peribronchial and perivascular inflammatory cells from lung sections revealed more severe lung inflammation after the adoptive transfer of in *vitro* MDSCs (Figures 3C, D, S6). Multiple poly(I:C) administrations upregulated the proinflammatory cytokines, GM-CSF, IFN-α, MCP-1, TNF-α, and the anti-inflammatory cytokine IL-10 in BALF, which were further upregulated upon adoptive transfer of in *vitro* MDSCs (Figure 3E). The expression levels of other cytokines, such as G-CSF, IL-1β, IL-2, IL-4, IL-5, and IL-6, were barely detectable or no significant change (Figure S7). Thus, MDSCs appear to aggravate poly(I:C)-induced lung inflammation.

# 4 Discussion

Viral infections target the airway and alveolar epithelial cells, causing alveolar epithelial injury that can lead to acute respiratory distress syndrome and even death (3, 37). Although dysregulated immune responses are hallmarks of severe infectious diseases, it remains unclear as to which innate and adaptive immune cells are

10.3389/fimmu.2023.1243851

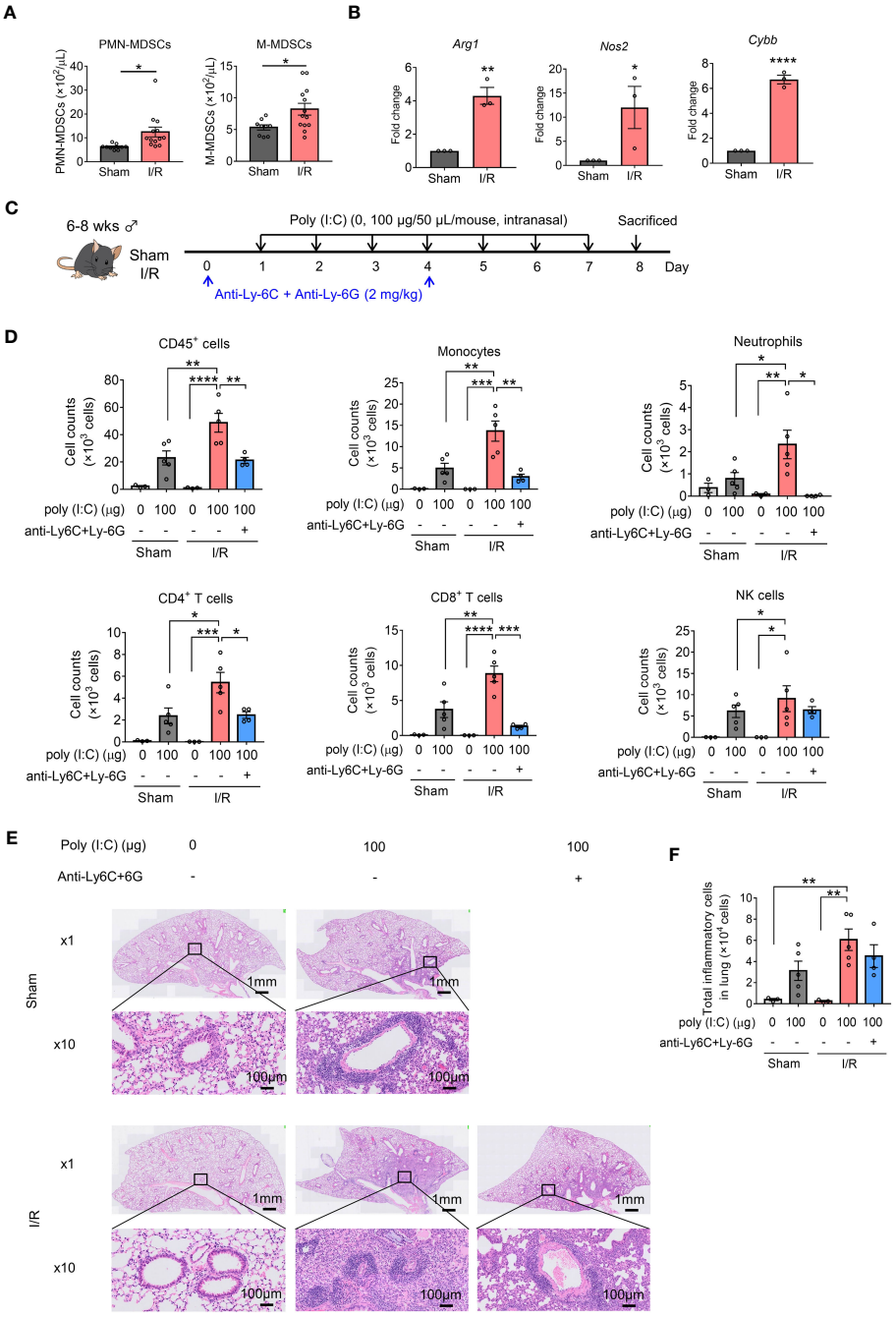


FIGURE 1
Myeloid-derived suppressor cells (MDSCs) aggravate poly(I:C)-induced lung inflammation in mice with renal ischemia/reperfusion (I/R) injury. **(A)** MDSC subsets in the blood were counted (mean ± SEM of two independent experiments; $n = 9$ in sham group, $n = 13$ in I/R group. Student's $t$-test: $^*p < 0.05$). **(B)** *Arg1*, *Nos2*, and *Cybb* mRNA expression in MDSCs ($CD11b^+Gr\text{-}1^+$) sorted from sham or I/R injury mouse spleens measured using qRT-PCR (mean ± SEM; $n = 3$ per group, Student's $t$-test: $^*p < 0.05$). **(C)** Mouse model of poly(I:C)-induced pneumonia established using an anti-Ly-6C/Ly-6G dosing schedule. **(D)** Total number of $CD45^+$ cells, monocytes, neutrophils, $CD4^+$ T cells, $CD8^+$ T cells, and NK cells in bronchoalveolar lavage fluid (BALF) assessed using flow cytometry (mean ± SEM; one-way ANOVA: $^*p < 0.05$, $^{**}p < 0.01$, $^{***}p < 0.001$, $^{****}p < 0.0001$). **(E)** Representative hematoxylin and eosin (H&E)-stained lung sections from Sham, I/R, and MDSC-depleted I/R groups at 1× and 10×. **(F)** Total inflammatory cells in H&E-stained lung sections identified using HALO AI (mean ± SEM; one-way ANOVA: $^{**}p < 0.01$).

critically involved in disease pathogenesis and which immunological mechanisms could be useful therapeutic targets. Higher morbidity and mortality rates in the elderly and in patients with chronic diseases may be related to increased MDSC levels. In this study, we showed that the frequency of MDSCs is increased before infection in older mice and in those with renal I/R injury, and is involved in the progression of viral pneumonia, leading to increased lung inflammation.

MDSCs exert immunosuppressive functions that may increase disease severity and cause clinical deterioration in patients with infectious diseases. However, MDSCs may also display features of

10.3389/fimmu.2023.1243851

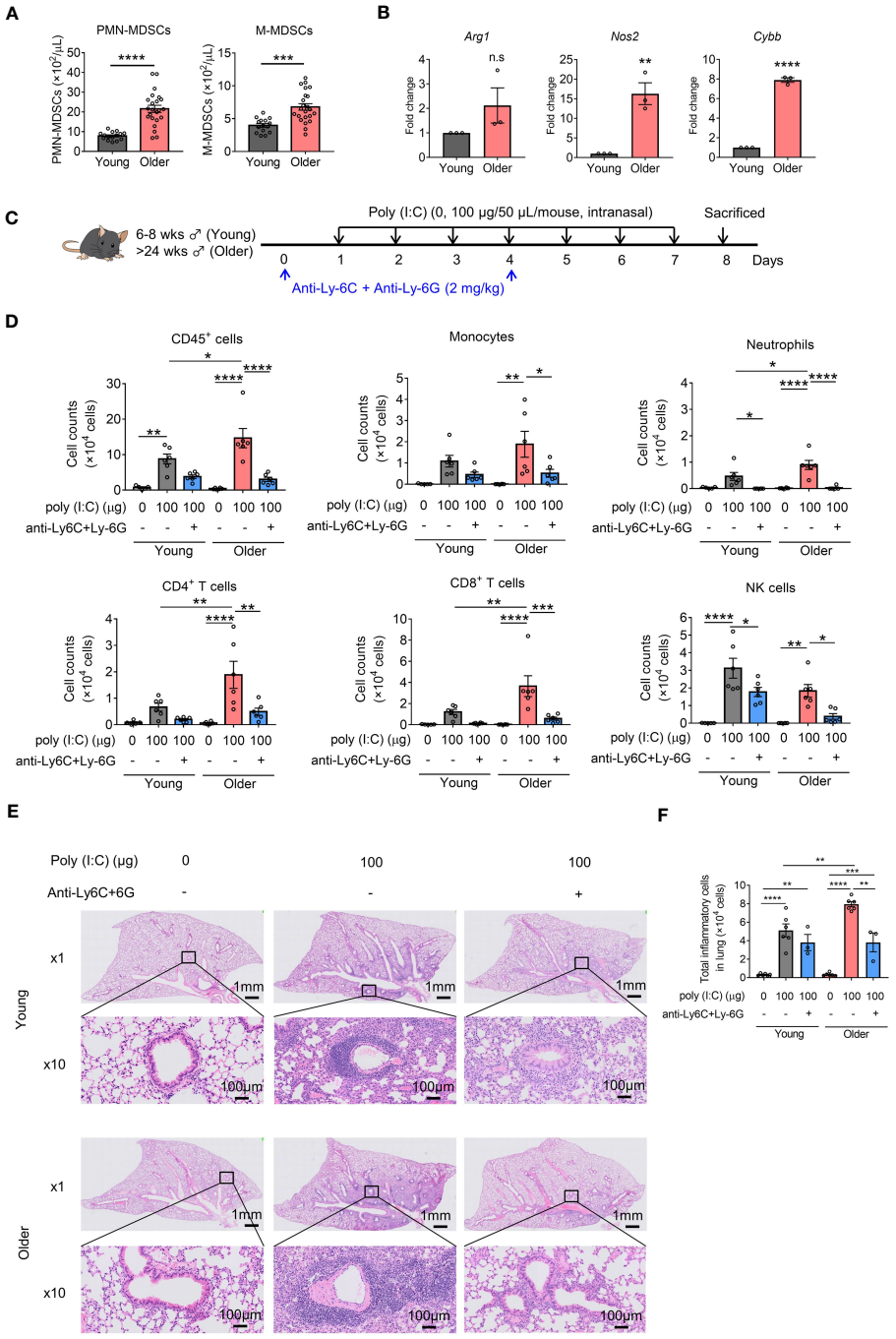


FIGURE 2
Myeloid-derived suppressor cells (MDSCs) aggravate poly(I:C)-induced lung inflammation in older mice. **(A)** MDSC subsets in the blood were counted (mean ± SEM of two independent experiments; $n$ = 15 in young, $n$ = 23 in older. Student's $t$-test: *$p < 0.05$). **(B)** *Arg1*, *Nos2*, and *Cybb* mRNA expression in MDSCs (CD11b$^+$Gr-1$^+$) sorted from young or older mouse spleens measured using qRT-PCR (mean ± SEM; $n$ = 3 per group. **(B)** Student's $t$-test: n.s., no significance; *$p < 0.05$). **(C)** Mouse model of poly(I:C)-induced pneumonia was established and treated with anti-Ly-6C/Ly-6G antibodies per the dosing schedule shown. **(D)** Total number of CD45$^+$ cells, monocytes, neutrophils, CD4$^+$ T cells, CD8$^+$ T cells, and NK cells in bronchoalveolar lavage fluid (BALF) assessed using flow cytometry (mean ± SEM; one-way ANOVA: *$p < 0.05$, **$p < 0.01$, ***$p < 0.001$, ****$p < 0.0001$). **(E)** Representative hematoxylin and eosin (H&E)-stained lung sections from young, older, and MDSC-depleted groups at 1x and 10x. **(F)** Total inflammatory cells in H&E-stained lung sections identified using HALO AI (mean ± SEM; one-way ANOVA: *$p < 0.05$, **$p < 0.01$, ***$p < 0.001$, ****$p < 0.0001$).

proinflammatory cells that contribute toward hyper-inflammation under certain conditions (22–24). Various factors secreted by inflamed tissues, such as GM-CSF, can promote the local recruitment of MDSCs from the circulatory system and promote their terminal differentiation into mature myeloid cells, as well as their activation to a proinflammatory phenotype with enhanced cytokine secretory capacity (38). These studies may explain the significant increase in the inflammatory cytokines, GM-CSF, IFN-

10.3389/fimmu.2023.1243851

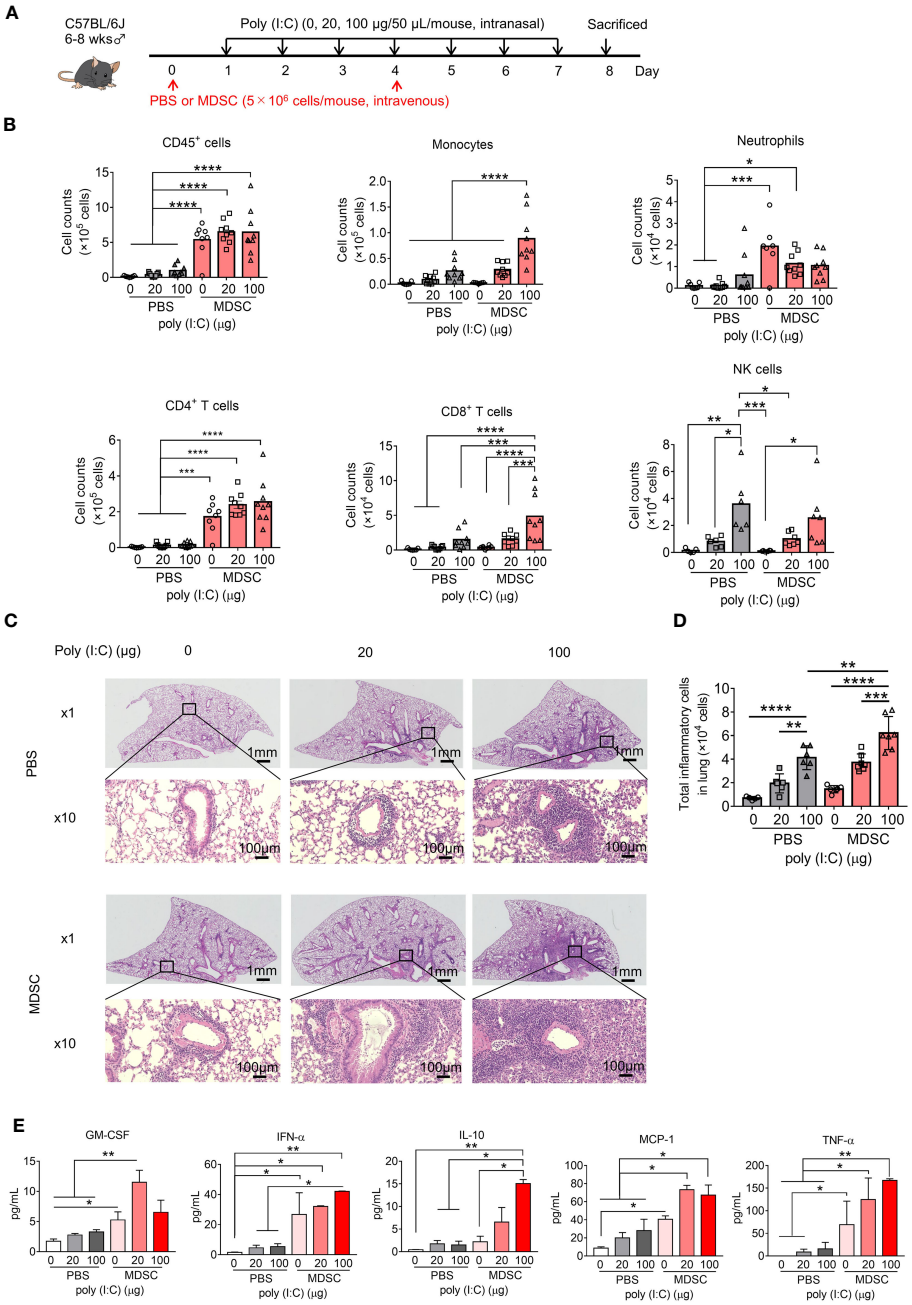


FIGURE 3
Adoptively transferred myeloid-derived suppressor cells (MDSCs) aggravate poly(I:C)-induced lung inflammation. **(A)** Mouse model of poly(I:C)-induced pneumonia established as shown with MDSC adoptive transfer. **(B)** Total number of $CD45^+$ cells, monocytes, neutrophils, $CD4^+$ T cells, $CD8^+$ T cells, and NK cells in bronchoalveolar lavage fluid (BALF) assessed using flow cytometry (mean ± SEM; one-way ANOVA: $*p < 0.05$, $**p < 0.01$, $***p < 0.001$, $****p < 0.0001$). **(C)** Representative H&E-stained lung sections from PBS or MDSC-transferred mice at 1x and 10x. **(D)** Total inflammatory cells in hematoxylin and eosin (H&E)-stained lung sections identified using HALO AI (mean ± SEM; one-way ANOVA: $**p < 0.01$, $***p < 0.001$). **(E)** Cytokines in BALF were analyzed using Bio-Plex (mean ± SEM; one-way ANOVA: $*p < 0.05$, $**p < 0.01$).

α, MCP-1, and TNF-α, observed in our study following the adoptive transfer of *in vitro* MDSCs in the absence of poly(I:C) challenge, suggesting that MDSCs may be a source of these cytokines. Consequently, MDSCs are probably dominant pathogenic factors in infectious diseases that drive exaggerated inflammation and the migration of immune cells into the lung. Furthermore, the MDSC transfer plus poly(I:C) administration group exhibited elevated levels of IL-10, an anti-inflammatory cytokine that plays a pivotal role in maintaining immune homeostasis by facilitating the clearance of infection (39). Because IL-10 is often induced together with proinflammatory cytokines, and provides an endogenous feedback to inhibit excessive inflammation (40), in our study, IL-10 induction would have occurred in a similar manner.

In older mice, all inflammatory cells analyzed in this study showed high infiltration in BALF when poly(I:C) was administered, whereas their infiltration was decreased by the depletion of $Ly\text{-}6C^+$

and Ly-6G$^+$ cells. Thus, Ly-6C$^+$ and/or Ly-6G$^+$ cells may be the key causes of inflammatory cell infiltration into the lungs of older individuals. In I/R-injured mice, NK-cell infiltration was increased following the depletion of Ly-6C$^+$ and Ly-6G$^+$ cells compared to that of other cells. Consistently, NK cell levels did not increase significantly with the adoptive transfer of in *vitro* MDSCs. I/R-injured mice were almost the same age as the young mice, suggesting that NK-cell infiltration is independent of MDSCs in young mice with or without disease. A massive increase in CD4$^+$ T cells and neutrophils was observed after the adoptive transfer of in *vitro* MDSCs; however, this change did not exacerbate pneumonia in the absence of poly(I:C), indicating that CD8$^+$ T cells, monocytes, and NK cells may play roles in the exacerbation of pneumonia. Recent studies have demonstrated that NK cells exert anti-SARS-CoV-2 activity but show defects in viral control, cytokine production, and cell-mediated cytotoxicity in patients with severe COVID-19 (41–43). Together with our results, these findings suggest that NK cells are a key factor in the deterioration of patients with pneumonia, in addition to MDSCs.

Because we found that MDSC depletion reduces poly(I:C)-induced lung inflammation in older mice and in those with I/R injury, our study highlights the potential of therapeutic approaches that aim to reduce the number of MDSCs. Preliminary studies have shown that a CCR5 inhibitor can alleviate SARS-CoV-2 plasma viremia in patients with COVID-19 (44). Targeting the CCL5/CCR5 axis can reduce the recruitment of MDSCs from the bone marrow to the lesion site (45); thus, COVID-19-related immunomodulatory disorders could be improved by targeting this pathway. The absence of HLA-DR is an important marker of human MDSCs and in one study it has been shown that IL-6 blockers can partially elevate HLA-DR expression, considering the decreased MDSC levels in patients with severe COVID-19 (46). Taken together, these data suggest that new approaches targeting MDSCs could be used to treat and prevent severe lung inflammation caused by COVID-19. It should be noted that although MDSC depletion in older mice reduced the severity of pneumonia to levels observed in young mice, MDSC depletion in young mice did not significantly improve pneumonia. Therefore, MDSC depletion may only attenuate the worsening of pneumonia in elderly patients or in those with underlying diseases.

The roles and mechanisms of M-MDSCs and PMN-MDSCs in diseases, including tumors and pneumonia, are distinct and require further exploration (22, 23). In our model, we observed a significant increase in the number of MDSCs in the blood, with PMN-MDSCs outnumbering M-MDSCs. However, it is important to note that in the BALF, the number of monocytes was significantly higher than that of neutrophils. This suggests that in our pneumonia model, more monocytes, including M-MDSCs, may be recruited to the site of lung inflammation. Further investigation is required to determine whether M-MDSCs play a more prominent role in exacerbating pneumonia.

Research on the relationships between MDSCs and acute or chronic viral infections is still in its infancy and has only begun to gain widespread attention since the COVID-19 pandemic. For instance, several recent studies have demonstrated an increase in the frequency of MDSCs in patients with COVID-19, which is related to immune regulation during infection and can be used as an indicator of the severity of COVID-19 (23). To our knowledge, no studies have yet reported the role of MDSCs in the progression of viral pneumonia in aging individuals and in those with chronic diseases. Although the details of the immune events and key mechanisms remain unclear, this study presents evidence that the increased MDSC profile present in older mice and in those with renal I/R injury exacerbates poly(I:C)-induced lung inflammation. In addition, we demonstrated that adoptively transferred MDSCs could worsen poly(I:C)-induced lung inflammation, indicating that MDSCs play a direct role in the pathogenesis of pneumonia. Further investigation is necessary to determine the applicability of our results to other related diseases. It should be noted that poly(I:C) does not effectively mimic the viral replication process; therefore, the effect of MDSCs on viral clearance requires further investigation. Due to the challenges associated with the separation and purification of cells, we were unable to perform in-depth functional and phenotypic analyses of lung MDSCs. Such analyses would have provided valuable insights into the mechanisms underlying the exacerbation of lung inflammation. Future studies should continue the investigation of the role of MDSCs in viral progression, their impact on the activation, exhaustion, and inhibition phenotypes of T and NK cells in the lungs, and their potential as a target for drug intervention in virus-infected mice or patients.

## Data availability statement

The original contributions presented in the study are included in the article/Supplementary Material. Further inquiries can be directed to the corresponding author.

## Ethics statement

The animal study was approved by The Animal Experiment Committee of Osaka University (approval number: Douyaku R03-7-2). The study was conducted in accordance with the local legislation and institutional requirements.

## Author contributions

ZX designed experiments and wrote the manuscript. ZX performed experiments and HZ assisted in data acquisition. MO and YF contributed toward the renal I/R injury model. NO helped with experimental design and assisted with discussions. MT conceptualized and supervised the study and wrote the manuscript. All authors contributed to the article and approved the submitted version.

## Funding

This work was supported in part by JSPS KAKENHI (Grant No. JP22H03533, Grants-in-aid for Scientific Research (B)) and a grant from The Drug Discovery Science Division, Open and

Transdisciplinary Research Initiatives, Osaka University (M.T.). This research was partially supported by the Zhejiang Provincial Natural Science Foundation of China (Grant No. LQ23H160001) (Z.X.). This research was also partially supported by the Platform Project for Supporting Drug Discovery and Life Science Research (Basis for Supporting Innovative Drug Discovery and Life Science Research (BINDS)) from AMED (Grant Nos. JP22ama121052 and JP22ama121054).

## Conflict of interest

The authors declare that the research was conducted in the absence of any commercial or financial relationships that could be construed as a potential conflict of interest.

## Publisher's note



## Supplementary material

The Supplementary Material for this article can be found online at: https://www.frontiersin.org/articles/10.3389/fimmu.2023.1243851/full#supplementary-material

## References

1. Subbarao K, Mahanty S. Respiratory virus infections: Understanding COVID-19. *Immunity* (2020) 52:905–9. doi: 10.1016/j.immuni.2020.05.004

2. Pagliano P, Sellitto C, Conti P, Ascione T, Esposito S. Characteristics of viral pneumonia in the COVID-19 era: an update. *Infection* (2021) 49:607–16. doi: 10.1007/s15010-021-01603-y

3. Meyer NJ, Gattinoni L, Calfee CS. Acute respiratory distress syndrome. *Lancet* (2021) 398:622–37. doi: 10.1016/S0140-6736(21)00439-6

4. Hu B, Guo H, Zhou P, Shi ZL. Characteristics of SARS-Cov-2 and COVID-19. *Nat Rev Microbiol* (2021) 19:141–54. doi: 10.1038/s41579-020-00459-7

5. Williamson EJ, Walker AJ, Bhaskaran K, Bacon S, Bates C, Morton CE, et al. Factors associated with COVID-19-related death using OpenSAFELY. *Nature* (2020) 584:430–6. doi: 10.1038/s41586-020-2521-4

6. Iaccarino G, Grassi G, Borghi C, Ferri C, Salvetti M, Volpe M, et al. Age and multimorbidity predict death among COVID-19 patients: Results of the SARS-RAS study of the Italian Society of Hypertension. *Hypertension* (2020) 76:366–72. doi: 10.1161/HYPERTENSIONAHA.120.15324

7. Roberts J, Pritchard AL, Treweeke AT, Rossi AG, Brace N, Cahill P, et al. Why is COVID-19 more severe in patients with diabetes? The role of angiotensin-converting enzyme 2, endothelial dysfunction and the immunoinflammatory system. *Front Cardiovasc Med* (2020) 7:629933. doi: 10.3389/fcvm.2020.629933

8. Mancusi C, Grassi G, Borghi C, Ferri C, Muiesan ML, Volpe M, et al. Clinical characteristics and outcomes of patients with COVID-19 infection: The results of the SARS-RAS study of the Italian Society of Hypertension. *High Blood Press Cardiovasc Prev* (2021) 28:5–11. doi: 10.1007/s40292-020-00429-3

9. Bailly L, Fabre R, Courjon J, Carles M, Dellamonica J, Pradier C. Obesity, diabetes, hypertension and severe outcomes among inpatients with coronavirus disease 2019: a nationwide study. *Clin Microbiol Infect* (2022) 28:114–23. doi: 10.1016/j.cmi.2021.09.010

10. Chan ASW, Ho JMC, Li JSF, Tam HL, Tang PMK. Impacts of COVID-19 pandemic on psychological well-being of older chronic kidney disease patients. *Front Med* (2021) 8:666973. doi: 10.3389/fmed.2021.666973

11. Hegde S, Leader AM, Merad M. MDSC: Markers, development, states, and unaddressed complexity. *Immunity* (2021) 54:875–84. doi: 10.1016/j.immuni.2021.04.004

12. Bronte V, Brandau S, Chen SH, Colombo MP, Frey AP, Greten TF, et al. Recommendations for myeloid-derived suppressor cell nomenclature and characterization standards. *Nat Commun* (2016) 7:12150. doi: 10.1038/ncomms12150

13. Veglia F, Perego M, Gabrilovich D. Myeloid-derived suppressor cells coming of age. *Nat Immunol* (2018) 19:108–19. doi: 10.1038/s41590-017-0022-x

14. Pawelec G, Verschoor CP, Ostrand-Rosenberg S. Myeloid-derived suppressor cells: Not only in tumor immunity. *Front Immunol* (2019) 10:1099. doi: 10.3389/fimmu.2019.01099

15. Pawelec G, Picard E, Bueno V, Verschoor CP, Ostrand-Rosenberg S. MDSCs, ageing and inflammageing. *Cell Immunol* (2021) 362:104297. doi: 10.1016/j.cellimm.2021.104297

16. Salminen A, Kaarniranta K, Kauppinen A. Immunosenescence: the potential role of myeloid-derived suppressor cells (MDSC) in age-related immune deficiency. *Cell Mol Life Sci* (2019) 76:1901–18. doi: 10.1007/s00018-019-03048-x

17. Zhang C, Wang S, Li JW, Zhang WT, Zheng L, Yang C, et al. The mTOR signal regulates myeloid-derived suppressor cells differentiation and immunosuppressive function in acute kidney injury. *Cell Death Dis* (2017) 8:e2695. doi: 10.1038/cddis.2017.86

18. Hsieh CC, Chang CC, Hsu YC, Lin CL. Immune modulation by myeloid-derived suppressor cells in diabetic kidney disease. *Int J Mol Sci* (2022) 23:13263. doi: 10.3390/ijms232113263

19. Salminen A. Increased immunosuppression impairs tissue homeostasis with aging and age-related diseases. *J Mol Med (Berl)* (2021) 99:1–20. doi: 10.1007/s00109-020-01988-7

20. Xing YF, Cai RM, Lin Q, Ye QJ, Ren JH, Yin LH, et al. Expansion of polymorphonuclear myeloid-derived suppressor cells in patients with end-stage renal disease may lead to infectious complications. *Kidney Int* (2017) 91:1236–42. doi: 10.1016/j.kint.2016.12.015

21. Pegues MA, McWilliams IL, Szalai AJ. C-reactive protein exacerbates renal ischemia-reperfusion injury: are myeloid-derived suppressor cells to blame? *Am J Physiol Renal Physiol* (2016) 311:F176–81. doi: 10.1152/ajprenal.00107.2016

22. Grassi G, Notari S, Gili S, Bordoni V, Casetti R, Cimini E, et al. Myeloid-derived suppressor cells in COVID-19: The paradox of good. *Front Immunol* (2022) 13:842949. doi: 10.3389/fimmu.2022.842949

23. Perfilyeva YV, Ostapchuk YO, Tleulieva R, Kali A, Abdolla N, Krasnoshtanov VK, et al. Myeloid-derived suppressor cells in COVID-19: A review. *Clin Immunol* (2022) 238:109024. doi: 10.1016/j.clim.2022.109024

24. Tomic S, Dokic J, Stevanovic D, Ilic N, Gruden-Movsesijan A, Dinic M, et al. Reduced expression of autophagy markers and expansion of myeloid-derived suppressor cells correlate with poor T cell response in severe COVID-19 patients. *Front Immunol* (2021) 12:614599. doi: 10.3389/fimmu.2021.614599

25. Koushki K, Salemi M, Miri SM, Arjeini Y, Keshavarz M, Ghaemi A. Role of myeloid-derived suppressor cells in viral respiratory infections; Hints for discovering therapeutic targets for COVID-19. *BioMed Pharmacother* (2021) 144:112346. doi: 10.1016/j.biopha.2021.112346

26. De Santo C, Salio M, Masri SH, Lee LY, Dong T, Speak AO, et al. Invariant NKT cells reduce the immunosuppressive activity of influenza A virus-induced myeloid-derived suppressor cells in mice and humans. *J Clin Invest* (2008) 118:4036–48. doi: 10.1172/JCI36264

27. Thakuri BKC, Zhang J, Zhao J, Nguyen LN, Nguyen LNT, Schank M, et al. HCV-associated exosomes upregulate RUNXOR and RUNX1 expressions to promote MDSC expansion and suppressive functions through STAT3-miR124 Axis. *Cells* (2020) 9:2715. doi: 10.3390/cells9122715

28. O'Connor MA, Rastad JL, Green WR. The role of myeloid-derived suppressor cells in viral infection. *Viral Immunol* (2017) 30:82–97. doi: 10.1089/vim.2016.0125

29. Miller MA, Stabenow JM, Parvathareddy J, Wodowski AJ, Fabrizio TP, Bina XR, et al. Visualization of murine intranasal dosing efficiency using luminescent *Francisella tularensis*: effect of instillation volume and form of anesthesia. *PloS One* (2012) 7:e31359. doi: 10.1371/journal.pone.0031359

30. Southam DS, Dolovich M, O'Byrne PM, Inman MD. Distribution of intranasal instillations in mice: effects of volume, time, body position, and anesthesia. *Am J Physiol Lung Cell Mol Physiol* (2002) 282:L833–9. doi: 10.1152/ajplung.00173.2001

31. Kim MG, Koo TY, Yan JJ, Lee E, Han KH, Jeong JC, et al. IL-2/anti-IL-2 complex attenuates renal ischemia-reperfusion injury through expansion of regulatory T cells. *J Am Soc Nephrol* (2013) 24:1529–36. doi: 10.1681/ASN.2012080784

32. Rabb H, Daniels F, O'Donnell M, Haq M, Saba SR, Keane W, et al. Pathophysiological role of T lymphocytes in renal ischemia-reperfusion injury in mice. *Am J Physiol Renal Physiol* (2000) 279:F525–31. doi: 10.1152/ajprenal.2000.279.3.F525

33. Vareille M, Kieninger E, Edwards MR, Regamey N. The airway epithelium: soldier in the fight against respiratory viruses. *Clin Microbiol Rev* (2011) 24:210–29. doi: 10.1128/CMR.00014-10

34. Cheng YS, Xu F. Anticancer function of polyinosinic-polycytidylic acid. *Cancer Biol Ther* (2010) 10:1219–23. doi: 10.4161/cbt.10.12.13450

35. Xie Z, Kawasaki T, Zhou H, Okuzaki D, Okada N, Tachibana M. Targeting GGT1 eliminates the tumor-promoting effect and enhanced immunosuppressive function of myeloid-derived suppressor cells caused by G-CSF. *Front Pharmacol* (2022) 13:873792. doi: 10.3389/fphar.2022.873792

36. Xie ZQ, Ikegami T, Ago Y, Okada N, Tachibana M. Valproic acid attenuates CCR2-dependent tumor infiltration of monocytic myeloid-derived suppressor cells, limiting tumor progression. *Oncoimmunology* (2020) 9:1734268. doi: 10.1080/2162402X.2020.1734268

37. van Riel D, den Bakker MA, Leijten LM, Chutinimitkul S, Munster VJ, de Wit E, et al. Seasonal and pandemic human influenza viruses attach better to human upper respiratory tract epithelium than avian influenza viruses. *Am J Pathol* (2010) 176:1614–8. doi: 10.2353/ajpath.2010.090949

38. Lang FM, Lee KM, Teijaro JR, Becher B, Hamilton JA. GM-CSF-based treatments in COVID-19: reconciling opposing therapeutic approaches. *Nat Rev Immunol* (2020) 20:507–14. doi: 10.1038/s41577-020-0357-7

39. Ip WKE, Hoshi N, Shouval DS, Snapper S, Medzhitov R. Anti-inflammatory effect of IL-10 mediated by metabolic reprogramming of macrophages. *Science* (2017) 356:513–9. doi: 10.1126/science.aal3535

40. Saraiva M, O'Garra A. The regulation of IL-10 production by immune cells. *Nat Rev Immunol* (2010) 10:170–81. doi: 10.1038/nri2711

41. Kramer B, Knoll R, Bonaguro L, ToVinh M, Raabe J, Astaburuaga-Garcia R, et al. Early IFN-alpha signatures and persistent dysfunction are distinguishing features of NK cells in severe COVID-19. *Immunity* (2021) 54:2650–2669 e14. doi: 10.1016/j.immuni.2021.09.002

42. Witkowski M, Tizian C, Ferreira-Gomes M, Niemeyer D, Jones TC, Heinrich F, et al. Untimely TGFbeta responses in COVID-19 limit antiviral functions of NK cells. *Nature* (2021) 600:295–301. doi: 10.1038/s41586-021-04142-6

43. Maucourant C, Filipovic I, Ponzetta A, Aleman S, Cornillet M, Hertwig L, et al. Natural killer cell immunotypes related to COVID-19 disease severity. *Sci Immunol* (2020) 5:eabd6832. doi: 10.1126/sciimmunol.abd6832

44. Patterson BK, Seethamraju H, Dhody K, Corley MJ, Kazempour K, Lalezari J, et al. CCR5 inhibition in critical COVID-19 patients decreases inflammatory cytokines, increases CD8 T-cells, and decreases SARS-CoV2 RNA in plasma by day 14. *Int J Infect Dis* (2021) 103:25–32. doi: 10.1016/j.ijid.2020.10.101

45. Umansky V, Blattner C, Gebhardt C, Utikal J. CCR5 in recruitment and activation of myeloid-derived suppressor cells in melanoma. *Cancer Immunol Immunother* (2017) 66:1015–23. doi: 10.1007/s00262-017-1988-9

46. Giamarellos-Bourboulis EJ, Netea MG, Rovina N, Akinosoglou K, Antoniadou A, Antonakos N, et al. Complex immune dysregulation in COVID-19 patients with severe respiratory failure. *Cell Host Microbe* (2020) 27:992–1000 e3. doi: 10.1016/j.chom.2020.04.009